Faceting in free dendritic growth

Mokhtar Adda Bedia and Martine Ben Amar
Laboratoire de Physique Statistique de l'Ecole Normale Supérieure, associé au CNRS et aux universités Paris VI et VII, 24 Rue Lhomond, 75231, Paris Cedex 05, France

(Received 25 January 1994; revised manuscript received 2 June 1994)

In recent crystal growth experiments [J. Maurer *et al.*, Europhys. Lett. **8**, 67 (1989)], faceted dendrites have been observed. These new diffusion-limited growing shapes have been described theoretically by means of the classical equations of dendritic growth and by using modified boundary conditions on the faceted parts of the interface. We propose a numerical treatment of the present set of equations in the limit of low undercooling. Steady faceted needle crystals are found with a growth rate selected by the amplitude of the cusp in a Wulff plot.

PACS number(s): 61.50.Cj, 68.70.+w, 64.70.Dv

I. INTRODUCTION

In many growth processes, crystal shapes show facets in specific directions [1,2]. When perpendicular to the **n** direction, these facets are observed for temperatures below $T_r(\mathbf{n})$, the roughening temperature for this orientation. In the case of dendritic growth, the experiments of Maurer *et al.* [2] on solidification of NH_4Br in water below the roughening temperature of the (110) direction have revealed the existence of faceted needle crystals. These are needle crystals with a general parabolic shape and facets close to the tip. In contrast to the completely rough needle-crystal case, where the quantity $\rho^2 v$ is a constant (ρ is the radius of curvature of the asymptotic parabola and v the rate along the growing direction), quantitative study of these new objects shown that $\rho^2 v$ now defines two plateaus, depending on whether v is greater or smaller than a certain velocity v_c. Moreover, the facet length Λ has been found to scale as $v^{-1/2}$, at least in the first plateau of smaller velocities where facets appear unambiguously. A theoretical explanation of these experimental observations has been proposed by Ben Amar and Pomeau [3]. They find that the scaling behaviors are well explained by a diffusion-limited-growth (DLG) model. They also argue that kinetic effects induced by the Franck-Read mechanism [4,5] maintain the degeneracy of the quantity $\rho^2 v$. These effects mainly contribute at low velocities and are irrelevant when the growth rate increases, so there is no need to introduce a roughening transition analysis to explain the existence of these two plateaus observed at low supersaturation. A complete treatment of this problem has not been performed to verify these predictions. The main questions still unanswered are (i) is it possible to find the exact shapes of faceted needle crystals using the DLG theory plus interfacial laws characteristic of faceting, and (ii) how does the introduction of facets affect the selection mechanism of the completely rough interfaces?

The theory of rough (=nonfaceted) growing needle crystals is well established in two models of solidification. For vanishing surface tension, Ivantsov [6] has shown that the solution of the needle-crystal problem yields a continuous set of parabolic shapes with a tip radius ρ, moving at a constant velocity v characterized by a given value $P(\Delta)=\rho v/2D$ of the Péclet number (Δ being the undercooling or the supersaturation and D the diffusion coefficient). Introducing the surface tension adds a new relation between the velocity and the tip radius of the Ivantsov parabola which removes this indefiniteness. This relation is given in terms of a nonlinear eigenvalue $C=4\rho^2 v/Dd_0$ [7,8] (the capillary length d_0 is of order of the lattice spacing). Previous theoretical and numerical works [9–14] have shown that the anisotropy of the surface tension is a necessary ingredient of steady growth and that, for each value of the anisotropy coefficient ε, there exists a discrete set of solutions C_n independent of the undercooling Δ.

In this paper, we examine two-dimensional faceted needle-crystal growth. The main problem we discuss is the existence of physical solutions within the DLG theory. Because of its practical interest we studied the simple case of steady-state growth at low undercooling. At zero capillary number on the rough parts of the interface, faceted dendrites do not exist. They cannot satisfy all the necessary conditions: tangential linkings between the facets and the rough parts and a continuous temperature (or concentration) field on the interface. A recent analytical [15] treatment confirms these findings. When one adds surface tension, a new degree of freedom appears, but also a new constraint: the vanishing of the first derivative of the profile function at the tip. The problem remains overconstrained and in a first numerical approach, we partially succeeded. In a previous treatment of faceted directional solidification [16], we did not encounter such numerical difficulties, probably because we treated the limit of large capillary numbers (C small) which is irrelevant for faceted dendritic growth. For the faceted directional solidification problem, we succeeded in showing [16] analytically and numerically that all the interfacial laws of faceting which follow from the model [3] [called the Ben Amar–Pomeau (BP) model in the following] are satisfied. But, for the faceted dendrite problem in the presence of capillary effects, the singularities of the "zero" surface tension set of solutions induced nu-

merical incertainties. So we decided to modify the numerical approach of this problem by working with, instead of a cusped surface tension, a strongly peaked surface stiffness around the facet orientations. In this way, we greatly simplified the free-boundary problem of faceted growth and obtained stable numerical results which satisfactorily converge when the peak is more and more pronounced. Within this model, we were able to show that steady faceted needle crystals exist and that the anisotropy coefficient is enough to select both the growth rate and the localization of the facets.

This paper is organized as follows. In Sec. II, we explain the BP model of faceted dendritic growth in situations far from equilibrium. In Sec. III, we explain the structure of our numerical treatment in both models. This leads to two different free-boundary problems: one with mixed boundary conditions at the interface and constraints at the facet ends, the second being a more classical one in this area. In Sec. IV, we summarize our numerical results and compare them to the experiment [2].

II. FACETED CRYSTAL SHAPES

At equilibrium, the crystal shape is entirely fixed [17] by its surface tension $\gamma(\theta)$, where θ is the polar angle of the surface normal $\mathbf{n}$. Once the Wulff plot [W plot, which represents $\gamma(\theta)$] is known, the crystal shape can be determined geometrically by the Wulff construction (W construction): it is homothetic to the convex envelope of the orthogonal lines to the $\mathbf{n}$ direction at a distance $\gamma(\theta)$. Moreover, the equilibrium condition of a curved interface fixes the local pressure variation ΔP in terms of the local curvature Ω:

$$\Delta P=\sigma(\theta)\Omega=\left[\gamma(\theta)+\frac{d^2\gamma(\theta)}{d\theta^2}\right]\Omega \ . \tag{1}$$

$\sigma(\theta)$ is called the surface stiffness. When the W plot exhibits a cusp in a specific direction θ_0, the W construction leads to a facet of length Λ given by

$$\Delta P\Lambda=\left.\frac{d\gamma}{d\theta}\right|_+-\left.\frac{d\gamma}{d\theta}\right|_- \ . \tag{2}$$

Besides, if the surface stiffness is positive on each side of the facet, the matching of the rough parts with the facet becomes tangential.

The case of nonequilibrium shapes is more complex. It is not easy to predict the shape of a growing crystal theoretically, since there is no equivalent of the W construction for this case. Moreover, one can wonder how to introduce, in a growth process, capillary effects which are responsible for the equilibrium crystal shape. In fact, usually [18–20] we assume the interface to be in a quasiequilibrium state which entails the assumption that the equilibrium interfacial laws (1) and (2) remain valid for the growth process. Then, when the pressure in the liquid phase is homogeneous, the Gibbs-Thomson-Herring (GTH) relation reads

$$-\phi=-\frac{\delta T}{T_m}L-\Delta\mu_i=\sigma(\theta)\Omega+\Delta\mu_k \ , \tag{3}$$

where L is the latent heat per unit volume of solid and δT is the local deviation of the liquid temperature from the melting temperature T_m. $\Delta\mu_i$ ($\Delta\mu_k$) is the liquid-solid chemical potential variation per unit volume of solid due to the presence of impurities (kinetic effects). The kinetic term $\Delta\mu_k$ measures the departure from equilibrium which slows down the growth. For rough interfaces, the attachment of the atoms at the interface is rather fast compared to the typical diffusion time except at high undercooling. Therefore this discontinuity is often neglected or reduced to a linear term $\beta\mathbf{v}\cdot\mathbf{n}$.

The GTH relation is valid on any smooth part of the crystal but is not valid at $\theta=\theta_0$ where $d^2\gamma(\theta)/d\theta^2$ is not defined and Ω vanishes. If we assume that, for faceted growth, the quasiequilibrium approximation remains valid, we need to modify the GTH relation according to Eq. (2) but we cannot impose a constant temperature (or concentration) on the facet. The profile of the faceted part is known, so the solidification free-boundary problem is overdetermined when one fixes the value of the diffusion field on each point of the facet. A way to handle this is to average Eq. (3) over the facet length [3]:

$$\int_\Lambda \phi\, ds=\langle\phi\rangle\Lambda=-\left[\left.\frac{d\gamma}{d\theta}\right|_+-\left.\frac{d\gamma}{d\theta}\right|_-\right]-\langle\Delta\mu_k\rangle\Lambda \ . \tag{4}$$

A similar relation has been established by Herring in the context of sintering [21]. As underlined in [3], the averaged law (4) is necessary to solve this free-boundary problem mathematically. The central question of this paper is whether this suffices to solve the problem of faceted crystal growth. It is also a way to fix the continuity of the temperature field on both sides of the facet.

The kinetic law $\Delta\mu_k$ which is a function of $\mathbf{v}\cdot\mathbf{n}$ depends on the facet growth mechanism [4,5]. For crystal growth in solutions, it is commonly thought that the Franck-Read mechanism is responsible for the facet growth process. Then the kinetic law depends linearly on the square root of v at very low growth rate and has a linear dependence on v when the growth rate increases. But, as emphasized in [3], due to the specific scaling laws of dendritic growth at low supersaturation, these effects contribute only at low velocities by increasing the facet length. In the following, we will choose a simple form for the W plot of a cubic crystal with two symmetric facets at $\pm\theta_0$:

$$\gamma(\theta)=\gamma_0\{1+\delta[|\sin(\theta-\theta_0)|+|\cos(\theta-\theta_0)|]\} \ , \tag{5}$$

where δ is the cusp coefficient. This choice defines our model I. This form gives a constant surface stiffness on the rough parts; also the facet length is related to the averaged field on the facet by

$$(\langle\phi\rangle+\langle\Delta\mu_k\rangle)\Lambda=-2\gamma_0\delta \ . \tag{6}$$

This relation shows that the facet length does not bring a new length scale, proving that the facet length scales as the tip radius. It also implies that in a nondynamical approach the shape of the faceted needle crystal should always be the same up to a dilation depending on the undercooling. As a consequence, the quantity $\Lambda^2 v$ is constant, which is in agreement with the experimental results of [2].

The representation of the surface tension by Eq. (5) leads to a Dirac distribution for the surface stiffness. It facilitates the analytical treatment of the faceted growth [15], but it complicates the numerical algorithm of the free-boundary problem. In order to obtain reliable numerical results, we decided to "soften" the Dirac distribution. We performed the calculations with two different representations of the surface stiffness:

$$\sigma(\theta)=\gamma_0\left[1+\frac{2\delta}{\pi}\frac{\alpha}{(\theta-\theta_0)^2+\alpha^2}\right], \tag{7a}$$

$$\sigma(\theta)=\gamma_0\left[1+\frac{2\delta}{\alpha\sqrt{\pi}}\exp-\left[\frac{\theta-\theta_0}{\alpha}\right]^2\right]. \tag{7b}$$

Note that Eqs. (7) are classical approximations among others for the Dirac distribution in the limit $\alpha\rightarrow 0$. Such representations, which define our model II, must give stable results independent both of α (when α is small) and of the chosen approximation of the Dirac distribution. This model is basically similar to [3] and it is only chosen for numerical convenience. Moreover, some microscopic models of faceting claim that the singularity in the surface stiffness does not represent the physical reality. A dynamical treatment of the roughening transition [22–24], which assumes a nucleation mechanism for the facet growth, has shown that in a growth process the cusp of the W plot is softened near the roughening transition. That is, cuspoidal singularities in the W plot can be replaced by pronounced dips in a smooth W plot [3]. The theory [22–24] also assumes a velocity-dependent cusp δ: the so called dynamical roughening transition which can explain the existence of the two plateaus as a consequence of the disappearance of both the cusp in the W plot and the facets when the velocity increases. The following analysis will not address all these problems, which require a full knowledge of the microscopic mechanism: we only focus on the possible existence of faceted dendrites within the DLG model.

III. NUMERICAL ANALYSIS

For the case of steady shapes, the liquid-solid interface profile is given by an integrodifferential equation which is well established both for the symmetrical [7] and the one-sided model [25]. Let us recall that the symmetrical model, which assumes the equality of the diffusion coefficient in both phases, is more adequate to describe solidification of a pure sample. The one-sided model, on the other hand, where the diffusion in the solid phase is neglected, describes the diffusion of impurities conveniently. The experimental observation [2] that there is no new length scale introduced by the appearance of facets, leads us to impose a parabolic asymptotic behavior for the faceted dendrite. Since we focus on low undercooling, the Pelcé-Pomeau procedure [8], which suppresses the undercooling from the initial equations, is still applicable. Then the integrodifferential equations satisfied by the nondimensional profile $\zeta(x)$ and the eigenvalue C are

(i) for the symmetrical model,

$$\phi(x)=-\frac{C}{4\pi}\int_{-\infty}^{+\infty}dt\,\ln\frac{(x-t)^2+[\zeta(x)-\zeta(t)]^2}{(x-t)^2+(x^2-t^2)^2}\ ; \tag{8a}$$

(ii) for the one-sided model,

$$\phi(x)=-\frac{C}{2\pi}\int_{-\infty}^{+\infty}dt\,\ln\frac{(x-t)^2+[\zeta(x)-\zeta(t)]^2}{(x-t)^2+(x^2-t^2)^2}+\frac{1}{\pi}\int_{-\infty}^{+\infty}dt\frac{[\zeta(x)-\zeta(t)]+(x-t)\zeta'(t)}{(x-t)^2+[\zeta(x)-\zeta(t)]^2}\phi(t)\ , \tag{8b}$$

where ζ' is the first derivative of ζ with respect to x. Note that we chose 2ρ as length unit so that the Ivantsov parabola, which fits the tail of the crystal, is $\zeta_{\rm iv}(x)=-x^2$. Using the definitions of the Péclet number and the nonlinear eigenvalue C, the values of the length scale ρ and the growth rate v are given by

$$\rho=\frac{C}{8P(\Delta)}d_0\ \text{ and }\ v=16\frac{[P(\Delta)]^2}{C}\frac{D}{d_0}\ . \tag{9}$$

It is important to emphasize that ρ does not represent the radius of curvature of the needle-crystal tip, but the radius of curvature of the Ivantsov asymptotic parabola. The difference between these two lengths can be important and one must be careful about the precise definition of ρ. Since the two models I and II imply different treatments, we will discuss them separately.

A. Model I

The function $\phi(x)$ represents the deviation from the Ivantsov field on the interface. On the rough parts of the interface, ϕ is given by the interface curvature term of the GTH equation. On the facets, the dimensionless field is the unknown variable, since the shape is predetermined. Thus, $\phi(x)$ can be written as follows: on the rough parts,

$$\phi(x)\equiv A(\theta)\frac{\zeta''(x)}{[1+\zeta'^2(x)]^{3/2}}\ , \tag{10a}$$

and on the facets,

$$\phi(x)\equiv\phi(x)\ , \tag{10b}$$

where $A(\theta)$ is the smooth part of the anisotropy factor of the surface tension [$A(\theta)=1$, when the surface tension is given by (5)]. For this problem, two physical constraints must be satisfied. First, because the surface stiffness is positive, the linkings of the different parts of the profile must be tangential, if one assumes that this property deduced from the equilibrium situation still holds. The second constraint is the continuity of the function $\phi(x)$, which follows from the continuity of the diffusion field along the interface.

The numerical procedure of this problem is based on the same approach used in the completely rough needle-crystal problem [11], with the difference that now the problem is *mixed*. On the one hand, on the rough parts the shape is the unknown variable; on the other hand, on the facet the dimensionless field is the unknown variable. For this problem, it is also convenient to fix the facet length Λ and to calculate the cusp coefficient δ by using Eq. (6). In the following, we will note the linking points

between the rough parts and the facet by x_b and x_e. We parametrize the interface as

$$\zeta(x)=-x^2+\frac{1}{C}\psi(x) \tag{11}$$

and discretize the interval $0\leq x\leq\infty$ into N points (with $x_b\equiv x_{n_b}$ and $x_e\equiv x_{n_e}$) by using a convenient change of variable. Furthermore, the curve is assumed to be symmetric around $x=0$ and we choose $\zeta(0)=0$. Then the remaining $(N-1)$ variables are the profile function points $\psi(x_i)$, with $2\leq i\leq n_b$ and $n_e+1\leq i\leq N$, the field points on the facet $\phi(x_i)$, with $n_b+1\leq i\leq n_e-1$, plus the coordinate x_b of the beginning of the facet. But one has $N+1$ equations: $N-1$ nonlinear equations obtained by evaluating the integral (8a) or (8b) at the observation points x_i $(i=1,\ldots,N-1)$ and two tangential matching conditions $\zeta'(x_i)=-\tan\theta_0$, for $i=n_b$ and $i=n_e$. Thus, there are two possible explanations: either the problem is ill posed and it needs more parameters, or there are two redundant equations. In the light of the analytical approach followed in [15] and in order to examine the first possibility, one may introduce a supplementary degree of freedom. In order to do this, one can introduce a nonphysical constant undercooling variation $\Delta\phi$ between the front and trailing rough parts. For that, one has to redefine the field $\phi(x)$ in the front rough part by

$$\phi(x)\equiv A(\theta)\frac{\zeta''(x)}{[1+\zeta'^2(x)]^{3/2}}+C\Delta\phi \quad \text{for } 0\leq x\leq x_b\ . \tag{12}$$

This new parameter will be our Nth variable. Of course, the physical solutions, if they exist, must correspond to a zero of $\Delta\phi$. Since we still have one supplementary equation and no other variables to introduce, one must suppress from the iterations one equation which should be redundant. In the following, we will choose to suppress the integral equation at $x=x_b$. Therefore we must verify after each iteration that this is really satisfied to a reasonable accuracy. Also, it is important to note that we did not impose the eigenvalue C to be an unknown parameter, because this variable must be used to impose a physical solution which must be smooth at $x=0$. This is done by looking for eigenvalues C that satisfy the condition $\zeta'(0)=0$.

B. Model II

The model II gives a classical integrodifferential equation which has been the subject of many treatments [9–14]. The difference with the work presented here comes from the choice of the anisotropy in the surface stiffness in Eq. (10a). Instead of using the multipole approximation $A(\theta)=1-\varepsilon\cos4\theta$, ε being the rough anisotropy coefficient, we take a sharply peaked function around $\theta_0=\pi/4$ [Eq. (7)]. Note that Eq. (10a) is valid everywhere since there is no real facet in this model. All the points are equivalent except the point zero at the tip where the condition $\zeta'(0)=0$ must be satisfied. This defines an equation for C. As can be noticed, we have thus greatly simplified the formulation of the previous mixed free-boundary problem. The only serious difficulty which can occur consists in the numerical stability of the results when the small parameter α goes to zero.

All integrals are performed to $O(1/N^2)$ and the solution is calculated using Newton's method starting from an initial numerical linearized solution around the Ivantsov parabola as explained in [11].

IV. NUMERICAL RESULTS

A. Results for model I

Vanishing surface tension limit

Physically, the zero surface tension limit has no sense for a faceted dendrite. However, let us assume that γ_0 is small (or C large), so that the curvature effects on the rough parts can be neglected. Formally, we obtain this limit by setting $C=1$, $\phi(x)=\Delta\phi$ in the front rough part, and $\phi(x)=0$ in the trailing one, everywhere in the above equations. As can be observed in Fig. 1, the numerical solution $\psi(x)$ is smooth everywhere. Unfortunately, as is shown in Fig. 2, the gap $\Delta\phi$ never vanishes, independently of the facet length. In order to obtain smooth functions $\psi(x)$, we have introduced a fictive unknown undercooling variation $\Delta\phi$ between the two rough parts. When one sets $\Delta\phi=0$ and eliminates the tangential matching condition at the point x_b (or at x_e) from the iterative equations, the correction to the Ivantsov parabola always presents a *singularity* at $x=x_b$ (or at $x=x_e$) (see Fig. 3). This "zero" surface tension limit has been investigated theoretically in the case of the one-sided model [15]. As seen in Figs. 1 and 3, there is good agreement between the analytical and numerical results. This comparison confirms that in this limit there are no solutions in both the symmetrical and the one-sided models of the DLG

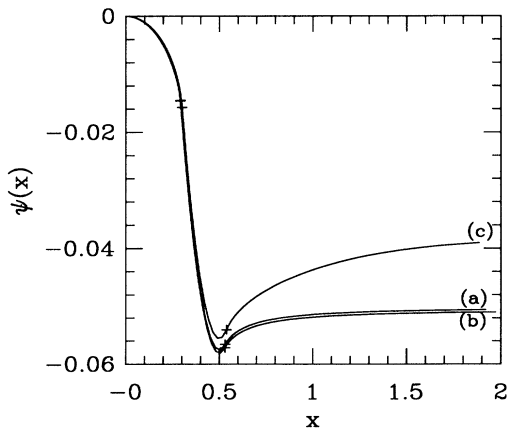

FIG. 1. Analytical (curve a) and numerical (curve b) solutions $\psi(x)$ for a vanishing surface tension, for $\Lambda=0.3383$ and $\theta_0=\pi/4$. The curve c corresponds to the correction $\psi(x)$ in the symmetrical model case for the same values of Λ and θ_0. These curves are obtained by assuming the existence of a variation $\Delta\phi$ between the two rough parts. The crosses show the beginning and the end of the facets.

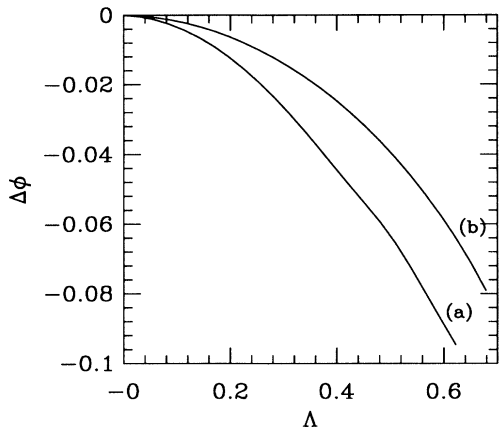

FIG. 2. Behavior of the undercooling variation $\Delta\phi$ as a function of the facet length Λ for (curve a) the one-sided and (curve b) the symmetrical model.

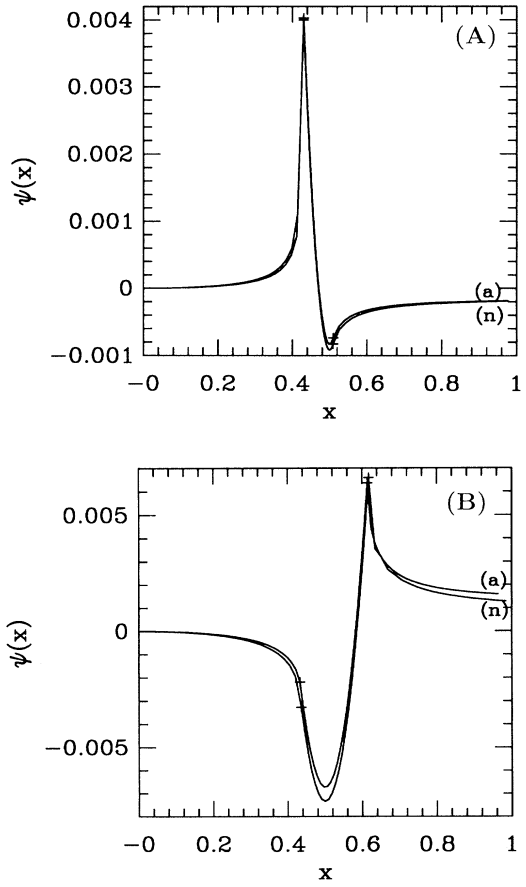

FIG. 3. (A) Analytical (curve a) and the numerical (curve n) solutions $\psi(x)$, for the one-sided model, for $\Lambda=0.1127$ and $\theta_0=\pi/4$ when $\Delta\phi=0$ is imposed and the profile singularity is chosen at $x=x_b$. (B) Analytical (curve a) and numerical (curve n) solutions $\psi(x)$, for the one-sided model, for $\Lambda=0.2571$ and $\theta_0=\pi/4$ when $\Delta\phi=0$ is imposed and the profile singularity is chosen at $x=x_e$.

theory. Let us now introduce the surface tension effects which perhaps may remove these singularities.

Nonvanishing surface tension

We will present in this section only the results obtained for the one-sided model. In fact, the conclusions below are not modified by the choice of the growth model. For this case, we first scanned a large interval of values for C ($100\leq C\leq 2000$) and also for Λ values ($0<\Lambda\leq 0.25/\cos\theta_0$). In these ranges, we did not find any physical solutions. Moreover, the absence of such solutions does not depend on the choice of θ_0. In Fig. 4, we plotted the functions $\Delta\phi=f(C)$ and $\zeta'(0)=g(C)$ for two different values of the facet length Λ and facet direction θ_0. It can be observed from the figures that the concentration gap $\Delta\phi$ and the shape slope at the origin $\zeta'(0)$ do not vanish simultaneously. Moreover, when $g(C)=0$ has solutions, for $\theta_0=\pi/4$, $f(C)$ does not change sign. When $f(C)=0$ has solutions, for $\theta_0=\pi/3$, $g(C)$ is always negative; it only vanishes for $C=\infty$.

The origin of the difference between the plots of $g(C)$

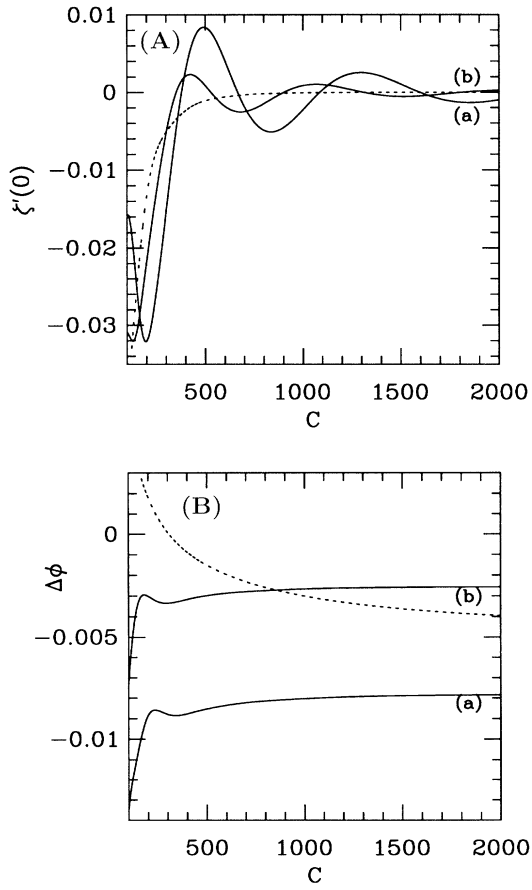

FIG. 4. (A) $\zeta'(0)=g(C)$ for $\Lambda=0.1/\cos\theta_0$ (curve a); for $\Lambda=0.05/\cos\theta_0$ (curve b), with $\theta_0=\pi/4$, and for $\Lambda=0.1/\cos\theta_0$ (dashed curve), with $\theta_0=\pi/3$. (B) $\Delta\phi=f(C)$ for $\Lambda=0.1/\cos\theta_0$ (curve a), for $\Lambda=0.05/\cos\theta_0$ (curve b), with $\theta_0=\pi/4$, and for $\Lambda=0.1/\cos\theta_0$ (dashed curve), with $\theta_0=\pi/3$.

for $\theta_0=\pi/3$ and $\pi/4$ can easily be explained by a comparison of the singularities that are involved. When introducing the surface tension effects in a completely rough problem, the curvature term introduces a singularity in the complex plane at the point $z=x+it=i/2$. The WKB analysis shows that, for suppressing the effect of this singularity, one must add another ingredient with a singularity which lies in the Stokes sector delimited by the Stokes line [26] defined by $\mathrm{Im}[S(z)]=0$, where Im denotes the imaginary part and $S(z)$ is given by

$$S(z)=\int_z^{i/2}(\tfrac{1}{2}+iu)^{1/2}(1+4u^2)^{1/4}du \ . \tag{13}$$

For the case of the rough interface, by assuming an anisotropic surface tension, one adds a singularity which lies in the interval $[0,\frac{1}{2}]$ on the imaginary axis. For a faceted problem, the facet itself entails a singularity which lies on the real "physical" axis. For both small facet length and small surface tension, this singularity is located at the point $x_0=\tan(\theta_0)/2$ [since $\zeta'(x_0)=-\tan\theta_0\approx-2x_0$]. By a simple numerical calculation, one finds that the Stokes line intersects with the real axis at the point $x_{\max}=\tan(\theta_{\max})/2$, with $\theta_{\max}\approx 56.45°$. So, in order to have solutions for this problem, one must have $x_0\le x_{\max}$ and consequently $\theta_0\le\theta_{\max}$. This is why the equation $g(C)=0$ exhibits solutions for $\theta_0=\pi/4(<\theta_{\max})$ and not for $\theta_0=\pi/3(>\theta_{\max})$.

One can wonder if there exists a physical parameter which, when taken into account, may cause the variable $\Delta\phi$ to vanish at the same points where $\zeta'(0)$ vanishes. Since we restricted ourselves to a Laplace approximation for the diffusion field, one may think of the Péclet number. However, as in many growth processes, this parameter has been shown not to be necessary for solving the problem of the possible existence of solutions. Another parameter which can play such a role is the rough anisotropy coefficient. However, when introducing this parameter in our problem the results remain the same. The rough anisotropy coefficient is not pertinent for a faceted problem. This numerical study shows that the solutions satisfying the physical constraint ($\Delta\phi=0$) exhibit singularities at the ends of the facet, which cannot be smoothed by a small amount of capillarity. One can expect that only strong surface tension may succeed in suppressing them as was demonstrated in [15]. Unfortunately, the numerical calculations for small C's or large Λ's has given some satisfactory results but with a large uncertainty. This is due to the fact that, in these limits, the front rough parts occupy regions that are very small, and consequently in the framework of this model the numerics cannot be so accurate there.

Fortunately, within the model II, all the difficulties explained above disappear and one is faced with a standard free-boundary problem [11]. The remaining difficulty

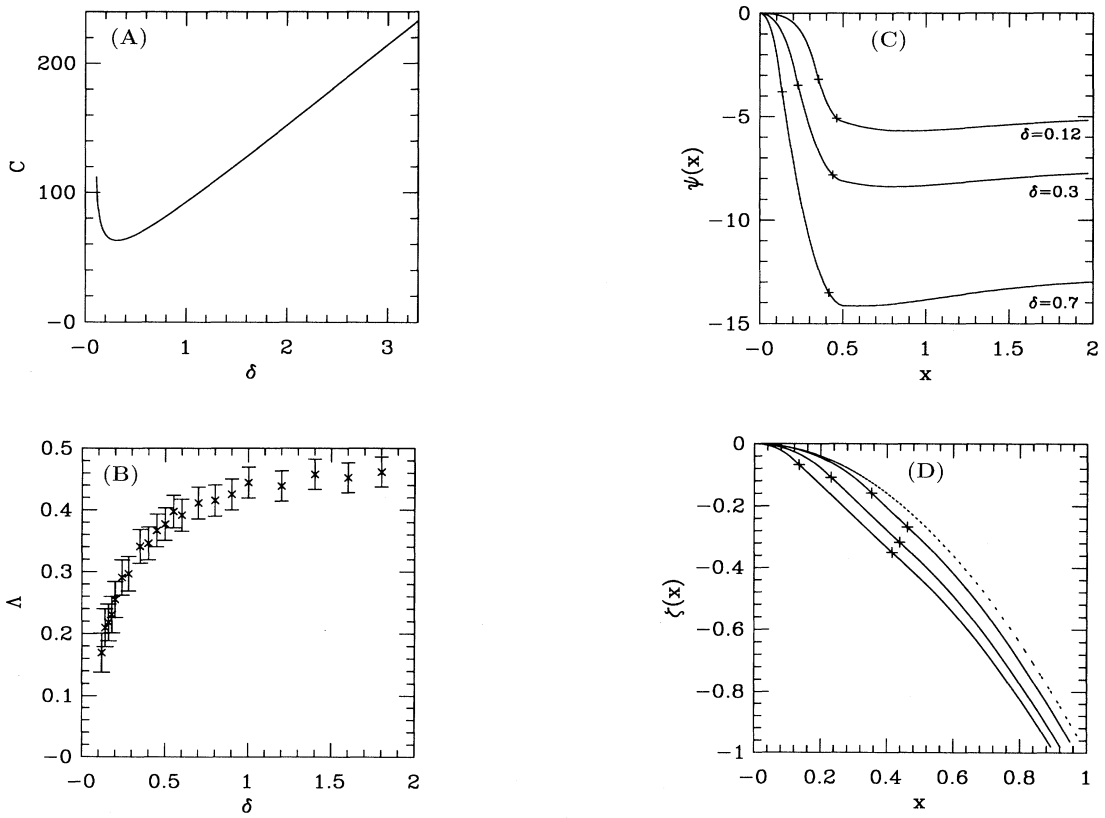

FIG. 5. (A) Selected first eigenvalue $C(\delta)$ for $\theta_0=\pi/4$ in the framework of model II. (B) Resulting "facet" length $\Lambda(\delta)$. The error bars are due to the fact that the points corresponding to $|\tan\theta-\tan\theta_0|=\alpha$ lie between two points of the discretized interface. (C) Corrections $\psi(x)$ to the Ivantsov parabola for selected shapes corresponding to different values of δ. (D) Selected shapes for the same values of δ as in (C). For comparison, the dashed curve is the Ivantsov parabola.

consists in the numerical stability of the results when the stiffness becomes more and more peaked around $\theta_0=\pi/4$; so when α goes to zero. These results are presented in the next section.

B. Results of model II

In model II, the profile shape is analytical everywhere as soon as the slope at the tip vanishes [$g(C)=0$]. This condition defines the eigenvalue C. So, except perhaps at the tip, all the points of the profile are equivalent and satisfy Eq. (10a). It is important to emphasize here that the introduction of this model is a pure numerical necessity. Therefore the physical solutions of a faceted dendrite must not depend either on the choice of the approximation for the Dirac distribution or on the magnitude of the parameter α, as long as α is small. This model has the advantage that all the points are equivalent, so the number of equations is equal to the number of the unknown variables. There is no need to introduce nonphysical additional parameters, since there are no discontinuities of the second derivative of the profile at the ends of the facet, as in model I. The only consequence of this approach is that the "facet" is not strictly flat but there is a part with a very small curvature. This is why a criterion has to be imposed for the definition of the facet end points. We choose to define the facet ends by the points which have $|\tan\theta-\tan\theta_0|=\alpha$. The results we present here are those obtained for the symmetrical model. In both approximations [Eq. (7)], the numerical solutions converged with α of order 10^{-3}, using the numerical scheme explained in [11]. The first and rather amazing result is the fact that the eigenvalue C is independent of the representation that is chosen for the Dirac distribution: Gaussian [Eq. (7b)], or Lorentzian [Eq. (7a)]. As is shown in Fig. 5(A), when the anisotropy coefficient δ increases from zero, the C eigenvalues decrease from infinity up to a minimum value, then increase again almost linearly with δ. The eigenvalue C is always large, even at the minimum: $C_{\min}\approx 62.8$. In principle and as is usually done in dendritic growth, this allows for a singular perturbation in the limit of vanishing δ and small "facets." The fact that the eigenvalue C does not depend on the surface stiffness approximation is a very puzzling observation. Of course, the singularities in the complex plane of x are independent of the model: $z=i/2$ and $z=1/2+i\varepsilon$ with ε small. Nevertheless, we know that the spectrum itself depends on the boundary layers around the singularities, which are different for the Lorentzian and Gaussian cases. This will be explained in a future publication. From a physical point of view, it is satisfying that the results do not depend on the details of the peaked surface stiffness. There is no difficulty in obtaining the different eigenvalues and profiles of the infinite discrete set but here we focus on the first eigenvalue, which is generally assumed to be the only relevant one.

When δ increases [Fig. 5(B)] the facet length increases and seems to saturate at a value around 0.47 for the Gaussian model. For the Lorentzian model, the results are qualitatively equivalent but the facet length is smaller for the same δ. Perhaps this is due to our definition of the facet ends which are more qualitative here. Finally, Figs. 5(C) and 5(D) exhibit profile functions for three different values of δ. Figure 5(D) shows that in this approximation we are really able to obtain numerically "facets" which reach appreciable sizes. Although we have not performed the calculations, it is clear that a similar representation can be used for the kinetic effects, which will lead to increasing the facet length at fixed δ.

C. Comparison with the experimental results

The faceted dendrite experiment on NH_4Br crystals [2] has revealed two plateaus which correspond to two different eigenvalues C. At low velocities, C is approximately 50; at the "highest" velocities C is about 100. From the experimental results, the nondimensioned facet length Λ turns out to be about 0.145. Since, for this experiment in solution, the one-sided model is more adequate, one can expect a difference of a factor of 2 for a thermal experiment, which would correspond to the symmetric model. As indicated in Fig. 5(B), the experimentally found value Λ suggests a rather small "effective" anisotropy coefficient: $0.11\leq\delta\leq 0.12$. Therefore, from Fig. 5(A), one obtains an estimate of the nonlinear eigenvalue C: $94.25\leq C\leq 111.84$. This corresponds perfectly to the first plateau in a thermal experiment. When the velocity of the dendrite increases, the relative importance of the kinetic effects decreases [3], so that the effective anisotropy coefficient δ decreases. This implies an increase of the eigenvalue C which could correspond to the second plateau observed experimentally. Note that the conclusions are opposite for a much more anisotropic material which would have a δ value greater than 0.3. Therefore our calculation is consistent with the experimental findings, although we have completely neglected three-dimensional effects. Of course, it is also consistent with a dynamical roughening transition around the critical velocity between the two plateaus. It cannot discriminate between these two interpretations which have been discussed in [3].

V. CONCLUSION

The main conclusion of this paper is that the DLG model of dendritic growth has no solutions in the limit of vanishing capillary number of the rough parts. In this limit we show that the model is overconstrained. Solutions can be obtained only if one relaxes some physical condition: for instance, if one allows the rough parts to have either an undercooling difference or nontangential matchings with the facets. We have not succeeded in proving unambiguously that solutions can exist for this model when surface tension is taken into account, contrary to our previous analysis for directional solidification [16]. When the surface stiffness is approximated by a peaked function (model II), the constraints of the free-boundary model I disappear and we get clear and unambiguous results: there is selection of the velocity of the needle crystal and selection of the facet ends, once the anisotropy δ of the W plot is known. Of course, if one knows the thermodynamic coefficient of the roughening transition (the W plot and the kinetic coefficients), one

can use this model and the algorithm derived from it to explain the existence of the two plateaus. Our modification of the BP model proves that steady faceted needle crystals can exist in the context of the DLG theory.

ACKNOWLEDGMENTS

We are grateful to D. Bonn and B. Moussallam for useful discussions. This work has been supported in part by ATP CNES-PIRMAT.

[1] K. A. Jackson and J. D. Hunt, Acta Metall. **13**, 1212 (1965); E. Raz, S. G. Lipson, and E. Polturak, Phys. Rev. A **40**, 1088 (1989).
[2] J. Maurer, B. Perrin, P. Bouissou, and P. Tabeling, Europhys. Lett. **8**, 67 (1989).
[3] M. Ben Amar and Y. Pomeau, Europhys. Lett. **6**, 609 (1988).
[4] W. K. Burton, N. Cabrera, and F. C. Franck, Philos. Trans. R. Soc. London Ser. A **243**, 299 (1951).
[5] J. D. Weeks and G. H. Gilmer, Adv. Chem. Phys. **40**, 157 (1979).
[6] G. P. Ivantsov, Dokl. Akad. Nauk. SSSR **58**, 567 (1947).
[7] G. C. Nash and M. E. Glicksman, Acta Metall. **22**, 1283 (1974).
[8] P. Pelcé and Y. Pomeau, Stud. Appl. Math. **74**, 245 (1986).
[9] M. Ben Amar and Y. Pomeau, Europhys. Lett. **2**, 307 (1986).
[10] D. Meiron, Phys. Rev. A **33**, 2704 (1986).
[11] M. Ben Amar and B. Moussallam, Physica D **25**, 155 (1987).
[12] D. Kessler and H. Levine, Phys. Rev. B **33**, 7678 (1986).
[13] A. Barbieri, D. C. Hong, and J. S. Langer, Phys. Rev. A **36**, 5353 (1987).
[14] D. Bensimon, P. Pelcé, and B. Shraiman, J. Phys. (Paris) **48**, 2081 (1987).
[15] M. Adda Bedia and V. Hakim, J. Phys. I (France) **4**, 383 (1994).
[16] M. Adda Bedia and M. Ben Amar, Phys. Rev. A **43**, 5702 (1991).
[17] L. D. Landau and E. Lifshitz, *Statistical Physics* (Pergamon, London, 1980).
[18] J. S. Langer, in *Chance and Matter,* edited by J. Souletie, J. Vannimenus, and R. Stora (North-Holland, Amsterdam, 1987).
[19] D. Kessler, J. Koplik, and H. Levine, Adv. Phys. **37**, 255 (1988).
[20] Y. Pomeau and M. Ben Amar, in *Solids Far From Equilibrium,* edited by C. Godrèche (Cambridge University Press, Cambridge, England, 1992).
[21] C. Herring, in *The Physics of Powder Metallurgy,* edited by W. E. Kingston (McGraw-Hill, New York, 1951).
[22] P. Nozières, in *Solids Far From Equilibrium* [20].
[23] F. Gallet, Thèse de Doctorat d'état de l'Université de Paris VI, 1986.
[24] P. Nozières and F. Gallet, J. Phys. (Paris) **48**, 353 (1987).
[25] B. Caroli, C. Caroli, B. Roulet, and J. S. Langer, Phys. Rev. A **33**, 442 (1986).
[26] S. Tanveer, Phys. Rev. A **40**, 4756 (1989).